High temperature–high pressure thermal conductivity of argon

Mahesh C. Aggarwal and George S. Springer

Department of Mechanical Engineering, The University of Michigan, Ann Arbor, Michigan 48109
(Received 3 July 1978)

A conductivity column-type apparatus was built and tested for measuring the thermal conductivities of gases at high temperatures and at high pressures. Two columns of different lengths were used in order to minimize end effects. The temperature and pressure limits were established below which multicellular convection cells did not form inside the column. The thermal conductivities of argon were measured in the temperature range 400 to 750 K and in the pressure range 0.1 to 8 MPa. The data were correlated by the expression

$$\lambda = (aT^b)\left[1 + A\left(\frac{P-P_0}{P_0}\right) + B\left(\frac{P-P_0}{P_0}\right)^2 + C\left(\frac{P-P_0}{P_0}\right)^3\right],$$

where $a = 0.2678\times10^{-3}$, $b = 0.7401$, $A = 0.2839\times10^{-4}$, $B = 0.1650\times10^{-4}$, $C = -0.1065\times10^{-6}$, $p_0 = 0.1$ MPa, and λ is in $\mathrm{W\,m^{-1}K^{-1}}$, T in K, and P in MPa. The thermal conductivity values obtained were compared with (1) existing data, (2) with results of viscosity measurements by means of the Eucken factor, and (3) with theoretical predictions based on a model for nonattracting rigid spherical molecules.

I. INTRODUCTION

Only a small fraction of the existing measurements of thermal conductivities of gases have been taken both at high temperatures and at high pressures. The majority of the experimental data reported in the literature were obtained at approximate atmospheric pressure (0.1 MPa). As the pressure increases, the number of data available proportionately decreases. This is likely due to the difficulties encountered during high temperature–high pressure experiments. The objective of this investigation was therefore to design an apparatus capable of measuring accurately thermal conductivities of gases at high temperatures and at high pressures, and to use the apparatus to measure the thermal conductivities of selected gases.

A conductivity column type apparatus was used in this investigation. The recent, successful use of this type of apparatus for measuring the thermal conductivities of gases at high temperatures and at low pressures (~0.1 MPa) (e.g., see the summaries in Refs. 1 and 2) warrants its extension to measurements at high temperatures and at high pressures.

Description of the apparatus and data for argon are presented here. Data for ethylene and propane are given in the following paper.

II. EXPERIMENTAL

In the tests conducted, the heat transfer $\bar{Q}_m$ from a fine tungsten wire filament suspended coaxially in a vertical cylinder was measured. In such an arrangement, often referred to as a conductivity column, heat is transferred from the filament by conduction $\bar{Q}_\lambda$, by radiation $\bar{Q}_r$, by convection through the gas $\bar{Q}_c$, and by conduction through the ends of the filament $\bar{Q}_e$:

$$\bar{Q}_m = \bar{Q}_\lambda + \bar{Q}_r + \bar{Q}_c + \bar{Q}_e \,. \tag{1}$$

To determine the thermal conductivity, the amount of heat conducted through the gas $\bar{Q}_\lambda$ must be known. In order to determine $\bar{Q}_\lambda$ from the measured value of $\bar{Q}_m$, the values of $\bar{Q}_r$, $\bar{Q}_c$, and $\bar{Q}_e$ must be known. As is explained in Sec. III, $\bar{Q}_r$ and $\bar{Q}_e$ can be estimated. The amount of heat loss from the filament due to convection must be minimized or eliminated.

Due to the temperature difference between the filament and the outer cylinder, the gas moves upward near the filament and downward in the outer portion of the column. In addition to this "primary" motion, multicellular convection may also occur inside the column. It has been shown[3] that, in the presence of only the primary motion, the heat convected from the filament becomes negligible compared to the conductive heat transfer at some distance from each end of the column. This distance (referred to as penetration depth) can be approximated by[3]

$$Z_p = \frac{D(Ra)}{7670} \qquad (Ra \geq 7670)\,, \tag{2}$$

where D is the inner diameter of the outer cylinder and Ra is the Rayleigh number defined as

$$Ra = \frac{g\rho^2 \Delta T D^3}{\eta^2 \bar{T}} \left.\frac{c_p \eta}{\lambda}\right|_{T=\bar{T}} . \tag{3}$$

g is acceleration due to gravity, ΔT is the temperature difference between the filament and the inside diameter of the outer cylinder, ρ is the density, η is the viscosity, c_p is the specific heat at constant pressure, λ is the thermal conductivity, and $\bar{T}$ is the average temperature of the gas.[4]

In order to select the inside diameter of the outer cylinder (column), two opposing requirements had to be met. First, it was necessary that the inside diameter be small enough to ensure a small value of Z_p [Eq. (2)]. Second, the diameter had to be large enough to enable an accurate centering of the filament. Taking into account these two opposing requirements as well as the availability of materials, the inside diameter of the column chosen was to be 0.104 cm. The filament diameter selected was 0.0102 cm. The penetration depth Z_p for this column was calculated as a function of pressure and filament temperature T_f for different gases (Fig. 1).

 0021-9606/79/083939-09$01.00

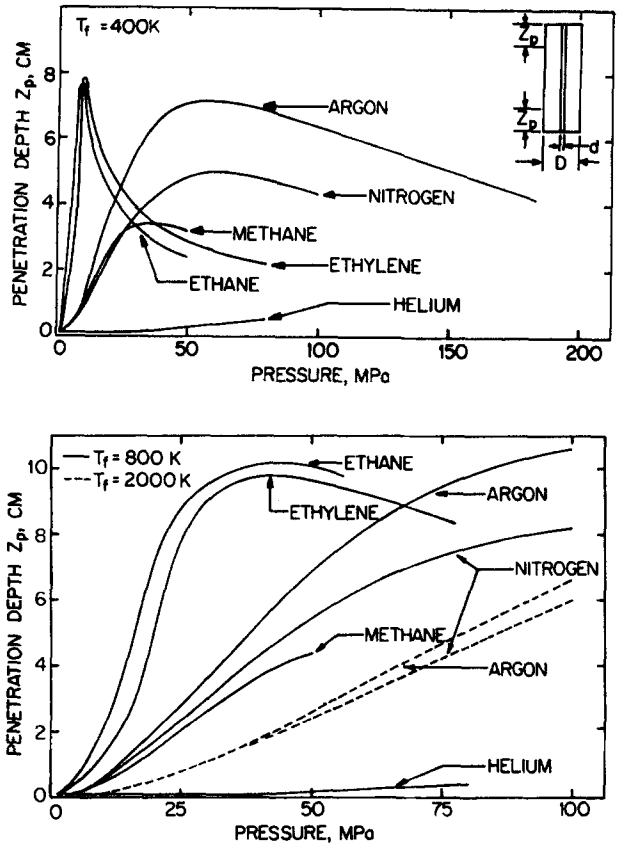

FIG. 1. Penetration depth as a function of pressure and filament temperature T_f at bath temperature $T_b = 300$ K ($D = 0.104$ cm, $d = 0.0102$ cm).

At high Rayleigh numbers, multicellular convection may form inside the column. Using numerical solutions to the Navier–Stokes and energy equations, Thomas and de Vahl Davis[5] analyzed the motion resulting from laminar convection inside a closed vertical annulus. According to their calculations, in annular cavities of length L, multicellular convection should not occur below the critical Rayleigh number

$$Ra_{crit} = 2.24\times10^{7}\left(\frac{c_p\eta}{\lambda}\right)^{0.5}\left(\frac{2L}{D-d}\right)^{2.27}\left(\frac{D}{d}\right)^{0.88}. \quad (4)$$

Critical Rayleigh numbers were calculated from Eq. (4) for the gases included in Fig. 1, and for the temperature and pressure ranges indicated in these figures. In all cases, the critical Rayleigh number was found to be $6-10\times10^{14}$. It was expected that as long as the Rayleigh number inside the column was less than this critical Rayleigh number, multicellular convection would not occur inside the column. The Rayleigh numbers prevailing during the experiments were estimated using Eq. (3). For the conditions given in Fig. 1, the calculations gave Rayleigh numbers on the order of 10^5, which are about nine orders of magnitude lower than the critical Rayleigh numbers. Therefore, multicellular convection should not occur in the present experiments. Unfortunately, the above expression [Eq. (4)] for the critical Rayleigh number was developed on the basis of information obtained at low pressure (0.1 MPa). At higher pressures, multicellular convection could occur at a lower Rayleigh number than that indicated by this expression. Therefore, the validity of this expression and the usefulness of the apparatus had to be checked by experiments. In fact, the data show (Sec. IV) that, at higher pressures, multicellular convection forms at Rayleigh numbers far below the critical Rayleigh numbers given by Eq. (4).

A. Test section

A schematic diagram of the test section is shown in Fig. 2. The conductivity column (0.318 cm o.d., 0.104 cm i.d.) was made of stainless steel 304, with a tolerance of ±0.0025 cm on the inside diameter. Each end of the column was fitted into a 6.668 cm high and 13.97 cm stainless steel block. A hole was drilled through the center of the block. The section of the hole adjoining the column was tapered to provide a smooth contact with the top of the column. Above the taper, the hole in the block was first narrowed to 0.397 cm and then was widened to 1.397 cm diameter. In this widened section, a "spacer" was placed to center the filament. The high pressure gas supply was connected to the test section through a hole drilled into the side of each block.

Two O-ring grooves were machined into the top of each block. The inner O ring, made of buna N, served as a high pressure seal, and the other one, made of viton, as a vacuum seal.

The blocks were sealed by 13.97 cm diam and 3.175 cm thick stainless steel caps. Commercially available high pressure electrical connectors were inserted into the test section through holes provided in the caps. The caps were fastened to the blocks by six bolts.

A copper layer 0.004 cm thick and 8.57 cm long was deposited by electrolysis on both ends of the filament. Each end of the filament was then pressed into a 3.5 cm long (0.025 cm i.d., and 0.081 cm o.d.) hypodermic needle. At the upper end of the column, this needle passed through a brass spacer. The radial position of

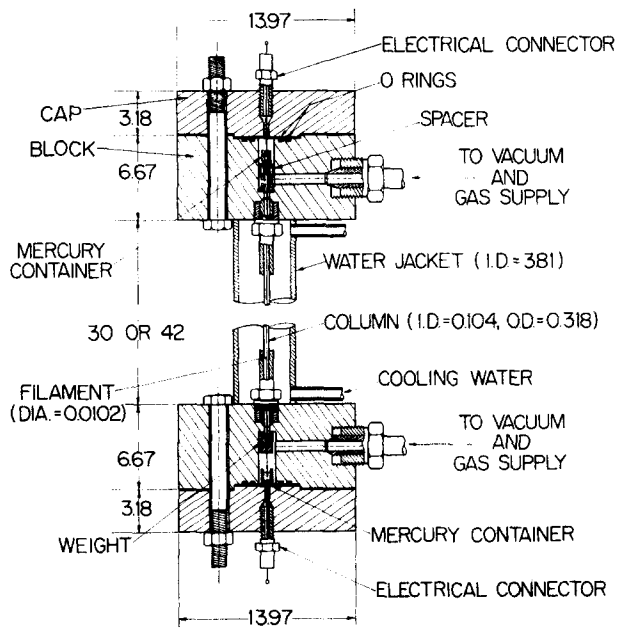

FIG. 2. Schematic diagram of the test section (all dimensions in cm).

this spacer, and accordingly the radial position of the filament, could be varied by two pins protruding radially from the spacer. The position of the pins were adjusted by set screws. The filament was roughly centered by first moving it in one direction until it made contact with the wall of the column, and then moving it in the opposite direction until it touched the wall at the other side of the column. The filament was set at half the distance of this movement. The procedure was repeated in a perpendicular direction. By this method, the filament was centered to within ±0.0051 cm of the central axis of the column. The values of thermal conductivity of argon were then checked at 0.1 MPa against the values predicted by kinetic theory. If this check revealed a discrepancy, the filament was adjusted until that discrepancy disappeared (Sec. III).

A Teflon container filled with mercury was placed above the spacer. A lead wire extending from the upper block reached into the mercury container, establishing electrical contact between the filament and the lead wire.

At the lower end of the filament, a 13 g weight was attached to the needle. The needle ended in a Teflon container filled with mercury and placed on the lower cap. The lead wire extending from the lower cap also reached into this container.

The conductivity column was surrounded by a 3.8 cm i.d. plexiglas tube. Water was circulated inside this tube to provide cooling for the column. The water temperature was measured continuously at its inlet and outlet by copper–constantan thermocouples.

The entire test section was mounted on a steel support fastened to the floor of the laboratory. The column was aligned to within 0.01° of the vertical.

In order to minimize end effects, two conductivity columns electrically connected in series were used in the tests. The two columns were identical except for their lengths which were 33 and 45 cm. The columns were attached to a high vacuum and a high pressure system.

B. High vacuum–high pressure systems

The high vacuum system was made of glass tubing. The apparatus was evacuated by a mechanical pump and a mercury diffusion pump. The pressure was measured with a McLeod gauge in the range of 1×10^{-4} to 25 mm Hg, and with an ionization gauge in the range of 10^{-8} to 10^{-4} mm Hg.

The high pressure system consisted of a diaphragm type compressor and stainless steel tubings. The pressure was measured by a U-tube mercury manometer and by four Bourdon tube type gages. High purity (99.998%) laboratory grade argon was used in the tests.

C. Electrical system

Power to the filaments was provided by dc power supplies. The voltage drop across each filament was measured by a high precision dc kilovolt standard. The currents through the filaments were determined by placing a precision standard resistor in series with each filament, and by measuring the voltage drop across this resistor by a high precision dc millivolt standard. The precision standard resistor (resistance R_0) was immersed in a constant temperature oil bath maintained at 25 °C.

Additional details of the apparatus may be found in Ref. 6.

III. TREATMENT OF THE DATA

Neglecting the convective heat transfer, in the presence of the gas, the heat conducted from the filament is

$$\overline{Q}_\lambda = \overline{Q}_m - (\overline{Q}_r + \overline{Q}_e) \ . \tag{5}$$

In vacuum ($\overline{Q}_\lambda^v \cong 0$), an energy balance for the filament gives

$$\overline{Q}_m^V = \overline{Q}_r^V + \overline{Q}_e^V \ , \tag{6}$$

where the superscript indicates measurement in vacuum. In the tests, the voltage drop across both the long and the short filaments, and the voltage drop across the standard resistor, were measured both in vacuum ($<2\times10^{-3}$ mm Hg) and in the presence of the gas. These measurements provided the values of filament current versus filament resistance, and the corresponding power losses in vacuum ($\overline{Q}_m^V$) and in the presence of the test gas ($\overline{Q}_m$).

It was assumed that the temperature distribution and end losses were the same for the short and long filaments.[3] It was further assumed that the radiation heat transfer was nearly the same in vacuum and in the presence of the gas ($\overline{Q}_r^V \cong \overline{Q}_r$). Accordingly, the heat conducted per unit length of the filament was expressed as

$$Q_\lambda = \frac{\overline{Q}_\lambda}{L_f} = \frac{(\overline{Q}_{mL} - \overline{Q}_{mS}) - (\overline{Q}_{mL}^V - \overline{Q}_{mS}^V)}{L_f} \ . \tag{7}$$

The subscripts L and S refer to the long and short filaments, respectively. L_f is the length of that portion of the filament which was at the uniform temperature T_f:

$$L_f = L_L - L_S \ . \tag{8}$$

All parameters appearing on the right hand side of Eq. (7) were determined experimentally. The data are presented in Table I. The heat conducted in vacuum $\overline{Q}_m^V$ was determined by smoothing graphically the data. The maximum difference between the measured and smoothed values was 0.2%. $\overline{Q}_m^V$ was always less than 8% of $\overline{Q}_m$. Thus, this procedure introduced a maximum error of 0.016% into Q_λ. The filament temperature was determined as follows:

The midfilament resistance R_f was defined as the resistance per unit length of that portion of the filament which was at the uniform temperature T_f:

$$R_f = \frac{\overline{R}_L - \overline{R}_S}{L_f} \ . \tag{9}$$

$\overline{R}_L$ and $\overline{R}_S$ are the total resistances of the long and short filaments, respectively. The relationship between midfilament resistance R_f and temperature T_f was established by mounting the filaments inside Pyrex columns and by measuring the midfilament temperature T_f with an optical pyrometer while recording the filament resistance. These measurements provided the relationship between R_f and T_f above 1100 K. The filament resistance at the water bath temperature was also obtained by the method described in Ref. 7. A linear plot of the

TABLE I. Tabulation of the argon data. Symbols are defined in conjunction with Eqs. (5)–(10). $L_S = 34.110$ cm and $L_L = 46.355$ cm.

P (MPa)	T_f (K)	$\bar{Q}_{ms}$ (W)	$\bar{Q}_{mL}$ (W)	$\bar{Q}^V_{ms}$ (W)	$\bar{Q}^V_{mL}$ (W)	Q_λ (W m^{-1})
0.10	378.5	0.978	1.613	0.0203	0.0343	5.07
	426.8	1.478	2.498	0.0315	0.0602	8.09
	495.0	2.177	3.788	0.0494	0.1058	12.70
	583.4	3.156	5.641	0.0873	0.2035	19.35
	690.2	4.492	8.226	0.1492	0.3877	28.55
	756.4	5.333	9.928	0.1930	0.5436	34.66
1.50	365.5	0.855	1.403	0.0176	0.0274	4.39
	414.5	1.324	2.235	0.0263	0.0502	7.25
	497.3	2.191	3.825	0.0492	0.1050	12.89
	607.0	3.413	6.176	0.0925	0.2279	21.46
	727.6	4.906	9.140	0.1623	0.4539	32.20
	820.5	6.183	11.712	0.2412	0.7208	41.24
3.00	385.7	1.055	1.761	0.0178	0.0351	5.62
	457.4	1.754	3.045	0.0302	0.0668	10.24
	533.3	2.573	4.574	0.0584	0.1341	15.72
	629.7	3.653	6.693	0.0976	0.2539	23.55
	745.3	5.138	9.639	0.1680	0.4886	34.14
	841.9	6.528	12.470	0.2465	0.7716	44.24
5.10	385.4	1.063	1.771	0.0195	0.0352	5.65
	439.9	1.635	2.785	0.0335	0.0599	9.18
	513.5	2.410	4.239	0.0537	0.1205	14.39
	598.8	3.403	6.134	0.0903	0.2187	21.26
	708.4	4.768	8.850	0.1473	0.4076	31.21
	835.7	6.595	12.523	0.2520	0.7735	44.15
6.48	383.5	1.054	1.761	0.0177	0.0325	5.65
	437.0	1.595	2.737	0.0290	0.0604	9.07
	507.9	2.312	4.103	0.0453	0.1074	14.12
	595.2	3.343	6.062	0.0819	0.2051	21.20
	704.5	4.668	8.719	0.1348	0.3835	31.05
	828.4	6.451	12.316	0.2304	0.7241	43.86
8.03	393.0	1.143	1.928	0.0181	0.0357	6.27
	448.7	1.722	2.981	0.0301	0.0659	9.99
	520.9	2.484	4.437	0.0474	0.1166	15.38
	614.7	3.548	6.513	0.0846	0.2221	23.09
	721.5	4.992	9.347	0.1473	0.4256	33.29
	816.6	6.333	12.083	0.2173	0.6800	43.18

measured values of R_f and the corresponding values of T_f provided the needed relationship between R_f and T_f within an average deviation of ± 0.25%.

The thermal conductivity of the gas was calculated from the Fourier equation

$$Q_\lambda = -2\pi r \lambda \frac{\partial T}{\partial R} \quad , \tag{10}$$

where T is the temperature at the radial position r. In order to determine λ as a function of T, Eq. (10) must be integrated. To perform this integration, the following relationship between λ and T was assumed[8]:

$$\lambda = aT^b \quad , \tag{11}$$

where a and b are constants which may depend on pressure. By substituting λ given by Eq. (11) into Eq. (10) and by integrating the resulting equation between $d/2$ and $D/2$, the following equation was obtained:

$$aT_f^b = \frac{(Q_\lambda/2\pi)\ln(D/d)}{[T_f/(1+b)][1-(T_b/T_f)^{1+b}]}(1+\lambda'+\lambda''+\lambda''') \, . \tag{12}$$

λ' is a correction for the temperature drop across the stainless steel column of thickness $w (w = 0.107$ cm) and thermal conductivity λ_{ss}:

$$\lambda' = \frac{\lambda(T_b)}{\lambda_{ss}} \frac{\ln(1+2w/D)}{\ln(D/d)} \quad . \tag{13}$$

λ'' is a correction for temperature jump at the filament surface[9]

$$\lambda'' = \left(\frac{2}{\gamma+1}\right)\left(\frac{\lambda}{\eta c_v}\right)_{T_f}\left(\frac{2-\alpha}{\alpha}\right)\frac{\bar{l}/(d/2)}{\ln(D/d)} \quad , \tag{14}$$

where γ is the ratio of specific heats, c_v is the specific heat at constant volume, α is the thermal accommodation coefficient at the tungsten filament, and $\bar{l}$ is the mean free path of the gas at the filament temperature. For argon, an accommodation coefficient of 0.8 was used in the calculation of λ''.[10]

λ''' is a correction for the thermal expansion of the filament

$$\lambda''' = \left[1-\left(\frac{T_b}{T_f}\right)^{1+b}\right]\left(\frac{T_f}{1+b}\right)\left(\frac{\beta}{1+\beta T_f}\right)\left[\frac{1}{2\ln(D/d)}-1\right] \, . \tag{15}$$

β is the coefficient of thermal expansion for tungsten (4.4×10^{-6} K^{-1}).[11] The total value of the corrections λ', λ'', and λ''' were found to be less than 0.5% of λ.

Equation (12) shows the relationship between Q_λ and the filament temperature T_f. At each pressure, the constants a and b were determined by drawing a smooth curve through the data given in Table I. From this curve, Q_λ were selected at nine values of T_f at 45 K intervals. These values of Q_λ and T_f were used to fit a least squares curve through Eq. (12), providing the values of a and b.

In order to evaluate the performance of the apparatus, the Eucken factor

$$f = \lambda/(\eta c_v) \tag{16}$$

was calculated using the values of λ determined experimentally at 0.1 MPa. The values of λ and c_v were taken from Refs. 12 and 13, respectively. The results are shown in Fig. 3. The values of f based on the measured

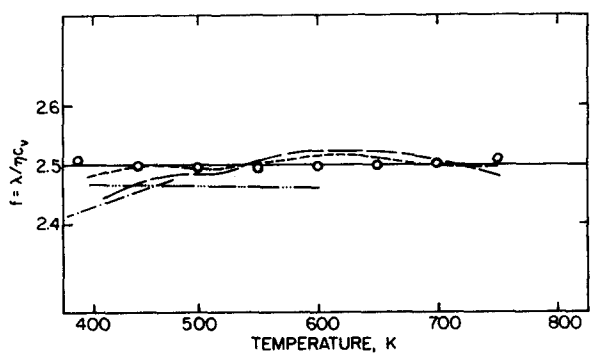

FIG. 3. Comparison between experimental and theoretical values of the Eucken factor for argon at 0.1 MPa. o present data; ----- Vargaftik[13]; -- Le Neindre *et al.*[15]; -·-·- Keyes and Vines[16]; -·- Moszynski and Singh[17]; — kinetic theory.[14]

TABLE II. Ranges of temperatures and pressure useful for the present apparatus.

Gas	Temperature (K)	Pressure (MPa)
Argon	400–750	0.1–8.0
Nitrogen	400–750	0.1–8.0
Helium	400–750	0.1–80.0
Methane	400–750	0.1–8.0
Ethane	400–750	0.1–2.0
Ethylene	400–750	0.1–2.8
Propane	400–725	0.1–0.6

thermal conductivity agreed to within ±0.4% with the values given by kinetic theory.[14] However, this close agreement between the experimental and theoretical values of f depended upon the proper centering of the filament inside the columns. Therefore, the procedure for centering the filament was repeated each time the filament was replaced.

IV. RESULTS

The thermal conductivity values of argon were measured in the temperature range 400–750 K and in the pressure range 0.1–8 MPa. The maximum temperature and pressure achieved in the experiments were limited to 750 K and 8 MPa, respectively. At higher temperatures and pressures, multicellular convection appeared in the column. This convection was evidenced by periodic fluctuations in the voltage drop across the filament. The filament was then mounted inside a Pyrex tube and periodic changes in color along the filament were observed. These color changes correspond to changes in filament temperature, giving further evidence of the existence of convection patterns. For argon at 8 MPa and 750 K, the Rayleigh number was about 5×10^4. This is a much lower value than the critical Rayleigh number Ra_{crit} predicted by Eq. (4). This lower Rayleigh number appears to be the actual critical Rayleigh number for this apparatus. Maximum temperatures and pressures which correspond to this Rayleigh number are listed in Table II.

The thermal conductivity values [i.e., the constants a and b in Eq. (11)] were evaluated from Eq. (12) at six different pressures. The value of $b=0.7401$ was found to be constant, independent of pressure. The values of a depended on pressure. The values of a are listed in Table III. In this table, thermal conductivities calculated from Eq. (11) are also given.

Note that the values of a and b at 0.1 MPa are different than those reported for argon by Springer and Wingeier,[8] because the temperature range in the present experiments was 400–750 K while the temperature range covered by Springer and Wingeier was 1000–2500 K.

The observation that b is independent of pressure suggests that the thermal conductivity may be expressed as

$$\lambda=\lambda(T,P)=\lambda_T(T)\cdot\lambda_P(P)\ , \tag{17}$$

where λ_T (W m^{-1} K^{-1}) is a function of temperature only, and λ_P is a dimensionless function of pressure only. For convenience, we took λ_T to be the thermal conductivity of argon at 0.1 MPa and represented this thermal conductivity by λ_0:

$$\lambda_T(T)=\lambda_0(T)=0.002678T^{0.7401}\ . \tag{18}$$

λ_P was expressed as

$$\lambda_P(P)=1+A\left(\frac{P-P_0}{P_0}\right)+B\left(\frac{P-P_0}{P_0}\right)^2+C\left(\frac{P-P_0}{P_0}\right)^3\ , \tag{19}$$

where P_0 is a reference pressure (0.1 MPa); A, B, and C are constants; and P is in MPa. Thus, the thermal conductivity of argon as a function of temperature and pressure was written as

$$\lambda=\lambda_0\left[1+A\left(\frac{P-P_0}{P_0}\right)+B\left(\frac{P-P_0}{P_0}\right)^2+C\left(\frac{P-P_0}{P_0}\right)^3\right]\ . \tag{20}$$

Using the experimental values of λ and λ_0 [Eqs. (11) and (18)] and the corresponding values of pressure P, a least squares curve was fitted through Eq. (20) giving $A=0.2839\times10^{-4}$, $B=0.1650\times10^{-4}$ and $C=-0.1065\times10^{-6}$. With these constants, Eq. (20) matched the data with a standard deviation of 5×10^{-6}. Fourth and fifth-order polynomials in pressure did not improve the correlation.

In Fig. 4, a comparison is given between the measured heat conduction (Table I) and the heat conduction calculated using thermal conductivity values given by Eq. (20). It can be seen from this figure that the maximum difference between the measured and calculated values of heat conduction was 0.7%.

TABLE III. The thermal conductivity of argon calculated from the expression $\lambda=aT^b$ ($b=0.7401$). The dimensions of a are such as to give λ in W m^{-1} K^{-1} when T is in K.

T(K) \ P(MPa)	0.1	1.50	3.00	5.10	6.48	8.03
			$\lambda\times10^3$ W m^{-1} K^{-1}			
400	22.57	22.64	22.86	23.25	23.53	23.79
450	24.63	24.68	24.92	25.38	25.63	25.94
500	26.62	26.68	26.93	27.45	27.69	28.04
550	28.57	28.64	28.90	29.46	29.71	30.10
600	30.47	30.56	30.83	31.42	31.68	32.09
650	32.33	32.45	32.72	33.31	33.62	34.04
700	34.15	34.29	34.58	35.14	35.51	35.94
750	35.94	36.10	36.39	36.92	37.36	37.78
$a\times10^3$	0.2678	0.2687	0.2710	0.2757	0.2789	0.2820

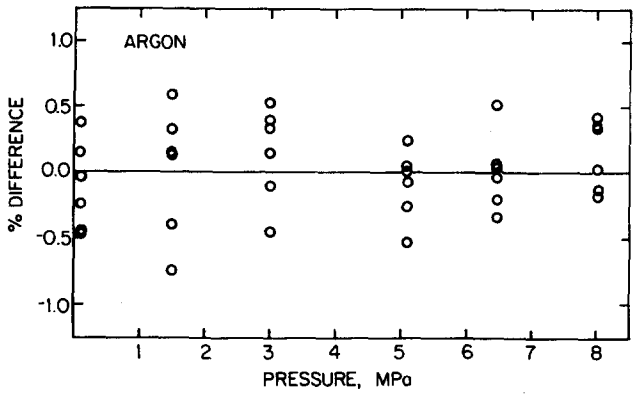

FIG. 4. Percent differences between the measured heat conduction and the heat conduction calculated using the thermal conductivity values given by Eq. (20). Points shown are for temperatures 400–750 K.

A detailed error analysis of the data was also made (Appendix I). The most probable random error in the data was estimated to range from 1.51% to 1.78%. The maximum systematic error was estimated to be 1.0%.

The thermal conductivity values obtained here were compared to the values reported in the literature. A large number of the thermal conductivity values for argon are available at 0.1 MPa ($T = 400$–750 K). Detailed comparison with the available data was not made at 0.1 MPa, because at this pressure close agreement was found between the theoretical and experimental Eucken factors (Fig. 3).

Thermal conductivity values for argon at high temperatures and high pressures were reported by Vargaftik,[13] Le Neindre and co-workers,[15] Keyes and Vines,[16] and Moszynski and Singh.[17]

Vargaftik reported thermal conductivity values for argon at pressures to 60 MPa over the temperature range of 90 to 1400 K. Measurements in the temperature range of 298 to 973 K and pressure range of 0.1 to 20 MPa were made by Le Neindre and co-workers. Keyes and Vines measured the thermal conductivity of argon in the pressure range of 0.1–14 MPa and temperature range of 413–621 K. Pressures to 160 MPa were reached by Moszynski and Singh in their measurements of the thermal conductivity of argon at 323, 373, 423, and 473 K.

The values of λ obtained in this investigation [Eq. (20)] were compared to those reported previously (Fig. 5). The results of the experiments presented here agree with those of Vargaftik to within 2.5%, the agreement being better at low pressures. The one exception is at 8 MPa and at 400 K, where the values differ by 4%. The present values agree with the values reported by Le Neindre *et al.* to within 2.4%.

Comparison between the present results and those of Keyes and Vines shows agreement to within 2.5%. It should be noted that in this comparison the equation for λ given by Keyes and Vines was used.

Moszynski and Singh expressed λ as a function of the density of argon in the density range of 0.6 to 533.5 amagat. The densities were converted to pressures using the relationship between density and pressure given by Michels and Wijker.[18] The present results and those reported by Moszynski and Singh agree to within 1.5%.

It is noted that the previous data scatter around the present λ values in a random manner. In order to assess the accuracies of the previous data, the Eucken factors were calculated using the thermal conductivity values reported in Refs. 13 and 15–17 (Fig. 3). The data of Vargaftik,[13] Le Neindre *et al.*,[15] and Moszynski and Singh[17] result in Eucken factors which change with temperature. The data of Keyes and Vines[16] yield Eucken factors which are about 2% lower than the kinetic theory value.

Finally, the experimental thermal conductivity values of argon [Eq. (20)] were compared to the thermal conductivity values calculated using Enskog's[14] model developed for nonattracting rigid spherical molecules (Appendix B). The maximum difference between the experimental and theoretical thermal conductivity values was 1.4% (Table IV).

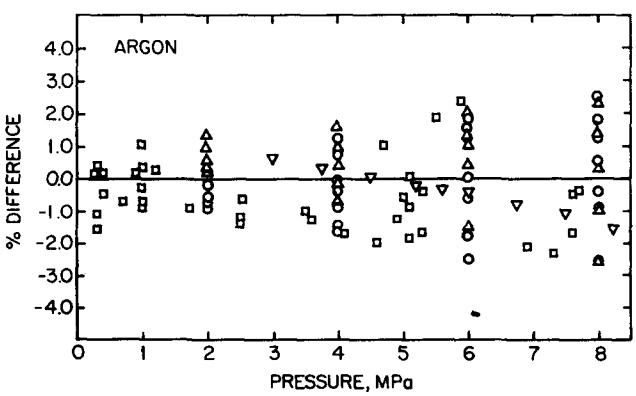

FIG. 5. Percent differences between the thermal conductivity values obtained in the present investigation [Eq. (20)] and the values reported by previous investigators. o Vargaftik[13] (400–750 K); Δ Keyes and Vines[16] (400–600 K); □ LeNeindre *et al.*[15] (413–748 K); ▽ Moszynski and Singh[17] (423 K).

TABLE IV. Percent differences between the thermal conductivity values for argon obtained in the present investigation [Eq. (20)] and the values obtained by Enskog theory[14] [Eq. (21)]: % Difference $= [(\lambda_{\text{Present}} - \lambda_{\text{Enskog}})/\lambda_{\text{Present}}] \times 100$.

T(K)	P(MPa)	$\lambda_{\text{Present}} \times 10^3$ (W m^{-1} K^{-1})	$\lambda_{\text{Enskog}} \times 10^3$ (W m^{-1} K^{-1})	% Difference
423.2	1.5	23.61	23.29	1.355
	3.0	23.82	23.91	−0.378
	5.0	24.20	24.28	−0.331
	6.5	24.51	24.57	−0.245
	8.0	24.77	24.90	−0.525
473.2	1.5	25.65	25.39	1.014
	3.0	25.87	25.88	−0.039
	5.0	26.29	26.22	0.266
	6.5	26.62	26.71	−0.338
	8.0	26.91	27.19	−1.041

ACKNOWLEDGMENT

This work was supported by the National Science Foundation.

APPENDIX A. ERROR ANALYSIS

If $y=y(x_1, x_2, \ldots, x_n)$, and P_{x1}, P_{x2}, $\ldots$, P_{x_n} are the probable errors associated with x_1, x_2, $\ldots$, x_n, then the most probable error associated with y (P_y) is given by[19]

$$P_y^2=\left(\frac{\partial y}{\partial x_1}\right)^2_{x_2,x_3,\ldots,x_n}\cdot Px_1^2+\left(\frac{\partial y}{\partial x_2}\right)^2_{x_1,x_3,\ldots,x_n}\cdot Px_2^2 + \cdots\left(\frac{\partial y}{\partial x_n}\right)^2_{x_1,x_2,\ldots,x_{n-1}}\cdot Px_n^2 . \quad \text{(A1)}$$

In order to estimate the most probable errors associated with the present experiments, Eq. (A1) was applied to each of the measurements. The filament resistance per unit length is

$$R_f=\frac{\bar{R}_L-\bar{R}_S}{L_L-L_S}=\frac{(V_L-V_S)(R_{\rm STD})}{(V_{\rm STD})(L_L-L_S)} , \quad \text{(A2)}$$

where V_L, V_S, and $V_{\rm STD}$ are the voltage drops across the long and short filaments and across the standard resistor of resistance $R_{\rm STD}$, respectively. By applying Eq. (A1) to (A2), we obtain

$$\frac{P_{R_f}^2}{R_f^2}=\frac{P_{V_L}^2}{V_L^2}+\frac{P_{V_S}^2}{V_S^2}+2\frac{P_{R\,\rm STD}^2}{V_{\rm STD}^2} + 2\frac{P_{V\,\rm STD}^2}{V_{\rm STD}^2}+\frac{P_{L_L}^2}{L_L^2}\left(\frac{L_L}{L_L-L_S}\right)^2+\frac{P_{L_S}^2}{L_S^2}\left(\frac{L_S}{L_L-L_S}\right)^2 . \quad \text{(A3)}$$

The probable errors associated with the various instruments as specified by the manufacturer were $P_{V_L}/V_L = 0.00007$, $P_{V_S}/V_S = 0.00007$, $P_{R\,\rm STD}/R_{\rm STD} = 0.00001$, $P_{V\,\rm STD}/V_{\rm STD} = 0.0001$, and $P_L/L = 0.00015$. The uncertainties introduced in reading the voltmeters were as follows: 0.0004–0.0001 for P_{V_L}/V_L, 0.00065–0.00018 for P_{V_S}/V_S, and 0.0018–0.00084 for $P_{V\,\rm STD}/V_{\rm STD}$. For the above values, Eq. (A3) yielded the most probable random error in R_f in the range of 0.17%–0.28%.

The heat conducted per unit length of the filament is

$$Q_\lambda=\frac{\bar{Q}_{mL}-\bar{Q}_{mS}}{L_L-L_S}-\frac{\bar{Q}^v_{mL}-\bar{Q}^v_{mS}}{L_L-L_S} . \quad \text{(A4)}$$

Following the foregoing procedure, the most probable random error in Q_λ was estimated to be in the range of 0.240%–0.396%.

In smoothing the current I versus resistance R curve in vacuum, 70% of the data points were within 0.1% of the smoothed curve. By applying the procedure described above, the total error caused by smoothing was found to be 0.14%. The heat transfer in a vacuum was at most 8% of the heat transfer in the presence of the gas. Thus, the error caused by smoothing the I versus R curve in vacuum introduced into λ a maximum random error of 0.01%.

The uncertainties introduced into T_f due to uncertainties in R_f (0.17%–0.28%), in pyrometer reading (~0.85%), and in relating R_f to T_f (0.25%) were 1.27% to 1.38%. The sum of the most probable random error in Q_λ and T_f (and consequently in λ) was in the range of 1.51%–1.78%.

The systematic error in the calculation of λ' depended on the test section geometry, on $\lambda(T_b)$, and on λ_{ss}. The column diameters were known within 2.5%, the filament diameters within 12%, and values of $\lambda(T_b)$ and λ_{ss} within 1.5% and 2.0%, respectively. The combined error due to these effects was approximately 8%. Since the maximum value of λ' was only 0.073% of λ, the systematic error introduced by λ' would have introduced into λ an error of only 0.006%.

The systematic error in the calculation of λ'' depended on the test section geometry (see above), γ, (λ/η_{c_v}), α, and $(\bar{l}/d)$. Values of γ and (λ/η_{c_v}) were known within 1.0%, α within 10%, and the Knudsen number $(\bar{l}/d)$ within 5%. The combined systematic error due to these effects was approximately 18%. Since the maximum value of λ'' was 0.53% of λ, the systematic error introduced by λ'' would have introduced into λ an error of 0.1%.

The systematic error in the calculation of λ''' depended on the test section geometry, β, T_b, T_f, and the constants a, b, and c. The values of β, T_b, and T_f were known within 1.5%, and a, b, and c within 0.5%. The combined systematic error due to these effects is approximately 4.5%. Since the maximum value of λ''' was 0.13% of λ, the systematic error introduced by λ''' would have introduced into λ an error of only 0.006%.

The systematic error in T_f (and consequently in λ) due to neglecting changes in the emissivity of the filament with temperature and absorption by the glass column was estimated to be 0.5%.

A maximum systematic error introduced by the filament being off center was estimated to be 0.4%. The sum of foregoing systematic errors was about 1.0%.

APPENDIX B. CALCULATION OF THE THERMAL CONDUCTIVITY OF ARGON USING THE ENSKOG MODEL

Enskog[14] developed the following equation to represent the effect of pressure on thermal conductivity for nonattracting rigid spherical molecules:

$$\lambda=\rho b_0\lambda_0(1/b_0\rho x+1.2+0.755 b_0\rho x) . \quad \text{(B1)}$$

$b_0=2\pi\sigma^3/3m$ is the second virial coefficient, σ the

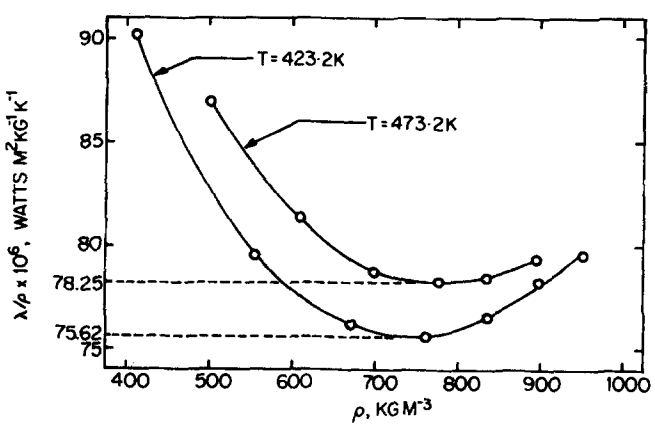

FIG. 6. λ/ρ versus the density ρ for argon. The values of λ and ρ are from Moszynski and Singh.[17]

TABLE V. The parameters $b_0\lambda_0$ and $b_0\rho x$ for argon calculated from Eqs. (B1) and (B3), respectively. The pVT data are from Vargaftik[13] ($P_c = 5$ MPa, $\rho_c = 536$ kg m^{-3}, $T_c = 150.86$ K, $Z_c = 0.2971$).

T(K)	P(MPa)	ρ(kg m^{-3})	$b_0\lambda_0 \times 10^6$ (W m^{+2} kg^{-1} K^{-1})	$\left(\frac{\partial P_R}{\partial T_R}\right)_\rho$	$b_0\rho \times 10^2$
423.2	1.5	16.934	26.63	0.1084	19.15
	3.0	34.001		0.2217	38.33
	5.0	56.559		0.3782	64.80
	6.5	72.253		0.4917	83.68
	8.0	90.099		0.6256	105.74
473.2	1.5	15.129	25.74	0.0965	16.18
	3.0	30.331		0.1966	32.46
	5.0	50.378		0.3336	54.64
	6.5	64.391		0.4326	69.81
	8.0	80.128		0.5470	87.14

diameter, and m the mass of the molecule. x is the value of the equilibrium radial distribution function at a distance σ from the center of an individual molecule. $b_0\rho x$ is called the Enskog modulus.

In order to calculate λ from Eq. (B1), the products $b_0\lambda_0$ and $b_0\rho x$ must be known. $b_0\lambda_0$ was evaluated as follows: First, Eq. (B1) was rewritten in the following form:

$$\lambda/\rho = b_0\lambda_0(1/b_0\rho x + 1.2 + 0.755 b_0\rho x) , \tag{B2}$$

and then Eq. (B2) was differentiated with respect to $b_0\rho x$ to obtain

$$\frac{d(\lambda/\rho)}{d(b_0\rho x)} = b_0\lambda_0\left[-\frac{1}{(b_0\rho x)^2} + 0.755\right] . \tag{B3}$$

From this equation, it may be seen that, by setting $d(\lambda/\rho)/d(b_0\rho x) = 0$, the minimum value of $\lambda/\rho[(\lambda/\rho)_{min}]$ results when $b_0\rho x = 1.151$. Therefore, this value of $b_0\rho x$ was substituted into Eq. (B2) to give

$$(\lambda/\rho)_{min} = b_0\lambda_0(2.938) . \tag{B4}$$

Equation (B4) can be rewritten as

$$b_0\lambda_0 = (\lambda/\rho)_{min}/2.938 . \tag{B5}$$

In order to calculate the value of $b_0\lambda_0$ from Eq. (B5), the value of $(\lambda/\rho)_{min}$ must be obtained. The value of $(\lambda/\rho)_{min}$ can be determined by plotting λ/ρ versus $b_0\rho x$ or ρ at the temperature of interest. The determination of this $(\lambda/\rho)_{min}$ requires that the experimental thermal conductivity values for argon be available for a range of pressure (density) determined by the temperature of interest. For temperature above 400 K, such data are available only for 423.2 and 473.2 K. Therefore, the values of $(\lambda/\rho)_{min}$ were obtained at $T = 423.2$ and $T = 473.2$ K by plotting the values of (λ/ρ) and the corresponding values of ρ as shown in Fig. 6. By substituting these values of $(\lambda/\rho)_{min}$ at 423.2 and 473.2 K into Eq. (B5), the corresponding values of the product $b_0\lambda_0$ at these same temperatures were obtained. These values are listed in Table V.

In order to calculate $b_0\rho x$, Enskog suggested the following relationship:

$$b_0\rho x = \frac{1}{\rho \mathfrak{R} T}\left[T\left(\frac{\partial P}{\partial T}\right)_\rho\right] - 1 . \tag{B6}$$

$\mathfrak{R}$ is a universal gas constant. Equation (B6) can be rewritten as

$$b_0\rho x = \frac{Z_c\rho_c}{\rho}\left(\frac{\partial P_R}{\partial T_R}\right)_\rho - 1 . \tag{B7}$$

Z_c is the critical compressibility factor, ρ_c is the critical density, and P_R and T_R are the reduced pressure and temperature, respectively. To calculate $b_0\rho x$ from Eq. (31), $(\partial P_R/\partial T_R)_\rho$ must be known. Values of P_R and T_R were obtained from experimental P–V–T data[13] at a constant density corresponding to the temperature and pressure at which the thermal conductivity of argon was to be calculated. For each density, the values of P_R were plotted against the corresponding values of T_R and a straight line was passed through these points. The slope of the straight line provided a value of $(\partial P_R/\partial T_R)_\rho$. For each density, the value of $(\partial P_R/\partial T_R)_\rho$ is tabulated in Table V. Actual graphs for P_R versus T_R are not plotted here but could be reproduced using the experimental data.[13] Once the values of $(\partial P_R/\partial T_R)_\rho$ at each desired density were known, the value of $b_0\rho x$ for each density was obtained from Eq. (B7). These are tabulated in Table V.

By substituting the values of $b_0\lambda_0$ and $b_0\rho x$ for each density (or pressure) into Eq. (B1), values of thermal conductivity for argon were calculated and tabulated in Table IV.

[1] V. K. Saxena and S. C. Saxena, J. Chem. Phys. **48**, 5662 (1968).

[2] F. M. Faubert and G. S. Springer, J. Chem. Phys. **57**, 2333 (1972).

[3] W. H. Lipkea and G. S. Springer, Int. J. Heat Mass Transfer **11**, 1341 (1968).

[4] S. H. P. Chen and S. C. Saxena, Report TR-E46, Department of Energy Engineering Report, University of Illinois at Chicago Circle (1972).

[5] R. W. Thomas and G. deVahl Davis, Proceedings of the International Conference on Heat Transfer, Paris-Versailles, 1970, Vol. 4, p. NC2.4.

[6] M. C. Aggarwal, Ph.D. Thesis, The University of Michigan, Ann Arbor (1978).

[7] L. B. Thomas and R. E. Brown, J. Chem. Phys. **18**, 1367 (1950).

[8] G. S. Springer and E. W. Wingeier, J. Chem. Phys. **59**, 2747 (1973).

[9] E. H. Kennard, *Kinetic Theory of Gases* (McGraw-Hill, New York, 1938).

[10] G. S. Springer, in *Advances in Heat Transfer*, edited by T. F. Irvine, Jr. and J. P. Hartnett (Academic, New York, 1971), Vol. 7, p. 163.

[11] R. Syre, *Handbook on the Properties of Niobium, Molybdenum, Tantalum, Tungsten, and Some of Their Alloys*, (AGARDOgraph N.A.T.O., Paris, 1965), Vol. 94, p. 171.

[12] J. Kestin, S. T. Ro, and W. Wakeham, Physica (Utrecht) **58**, 165 (1972).

[13] N. B. Vargaftik, *Tables on the Thermophysical Properties of Liquids and Gases* (Hemisphere, Washington, 1975), 2nd edition.

[14] J. O. Hirschfelder, C. F. Curtis, and R. B. Bird, *Molecular Theory of Gases and Liquids* (Wiley, New York, 1967).

[15]B. Le Neindre, R. Tufeu, P. Bury, P. Johannin, and B. Vodar, in *Thermal Conductivity*, edited by C. Y. Ho and R. E. Taylor (Plenum, New York, 1969), p. 75.
[16]F. G. Keyes and R. G. Vines, J. Heat Transfer **87**, 177 (1965).
[17]J. R. Moszynski and B. P. Singh, *Proceedings of the Sixth Symposium on Thermophysical Properties*, Atlanta Ga., (A.S.M.E., 1973), p. 22.
[18]A. Michels and H. K. Wijker, Physica (Utrecht) **15**, 627 (1949).
[19]H. Schenck, Jr., *Theories of Engineering Experimentation* (McGraw-Hill, New York, 1968), 2nd edition.